Available online at www.sciencedirect.com

SciVerse ScienceDirect

Ceramics International 39 (2013) 1511–1517

CERAMICS INTERNATIONAL

www.elsevier.com/locate/ceramint

# Facile synthesis of CdS nanoparticles photocatalyst with high performance

Fengjuan Chen, Yali Cao, Dianzeng Jia*, Xiaojuan Niu

*Key Laboratory of Advanced Functional Materials of Autonomous Region, Key Laboratory of Clean Energy Material and Technology of Ministry of Education, Institute of Applied Chemistry, Xinjiang University, 830046 Xinjiang, PR China*

Received 27 June 2012; received in revised form 28 July 2012; accepted 29 July 2012
Available online 6 August 2012

**Abstract**

A simple one-step solid-state reaction has been introduced to synthesize CdS nanoparticles. The as-prepared CdS product was characterized by X-ray powder diffraction (XRD), BET surface area measurement, field emission scanning electron microscopy (FESEM), transmission electron microscopy (TEM), particle size distribution (PSD) and UV–vis absorption spectrum. The experiment results reveal that the CdS product was composed of nanoparticles about 60 nm in diameter, of which specific surface area is 78.02 $m^2/g$. The photocatalysis results indicate that the CdS nanoparticles exhibit excellent photocatalytic activity for the degradation of rhodamine B under UV irradiation. Nearly 95% of rhodamine B was degraded after 60 min of irradiation, higher than that of P25, which is due to the large specific surface area and mesoporous structure.


*Keywords:* CdS; Nanoparticles; Photocatalysis; Solid-state reaction

## 1. Introduction

Environmental problems associated with organic pollutants promote the development of fundamental and applied research in the area of environment [1,2]. Hence, various methods have been developed to remove organic pollutants, like biodegradation, adsorption, and photocatalytic oxidation [3–5]. Among them, using semiconductor photocatalysis technology for degradation of organic pollutants has drawn an increasing interest, attributing to its great potentials, such as environmental friendly, low-cost and sustainable treatment. Although significant progress has been made, there is still much research needed to be undertaken, like the availability of highly efficient photocatalysts for water purification [6–8].

Among the various semiconductor materials, cadmium sulfide (CdS) has received considerable attention due to a large number of technical applications like photocatalysis, gas-sensing, photo-sensitive field emission switches and so on [9–11]. Especially, proper band potentials of CdS thermodynamic conditions for photocatalytic redox reaction, make it an efficient photocatalyst [12–14]. Recently, Wu et al. reported that CdS showed the highly efficient photocatalytic performance on reducing 4-nitroaniline [15]. Also, Luo et al. studied the photocatalytic activity of CdS hollow spheres and found they exhibited excellent photocatalytic activity for the photodegradation of Rhodamine B under UV irradiation [16].

In general, the photocatalytic activity of CdS is strongly dependent on its nanostructure. Owing to the efforts from many research groups, a variety of methods have been used to obtain CdS nanostructures, such as thermal evaporation method, solvothermal method, and thermal decomposition of a single-source precursor method and solid-state reaction [17–20]. Among these, the solid-state reaction method is an effective technique, which has the merits of environmentally friendly, simplicity, low-cost and high output. In recent years, our research group has adopted solid-state reaction to synthesize many semiconductor nanomaterials [21,22].

In this paper, CdS nanoparticles have been prepared by one-step solid-state reaction and characterized by XRD, BET, PSD, FESEM, TEM and UV analyses.

*Corresponding author. Tel.: +86 991 8583083; fax: +86 991 8580032.
*E-mail address:* jdz0991@gmail.com (D. Jia).

0272-8842/$ - see front matter © 2012 Elsevier Ltd and Techna Group S.r.l. All rights reserved.
http://dx.doi.org/10.1016/j.ceramint.2012.07.098

The photocatalytic performance of the CdS nanoparticles has also been extensively evaluated by the degradation of rhodamine B (RhB) under UV irradiation. The results demonstrated that CdS can be used as an efficient photocatalyst to degrade organic pollutants in the future.

## 2. Experimental section

### 2.1. Synthesis

All the reagents were analytically pure, and were used without further purification. In a typical synthesis, 10 mmol cadmium acetate ($Cd(CH_3COO)_2 \cdot 2H_2O$) was accurately weighed and ground for about 5 min, then 3 m L polyethylene glycol 400 (PEG 400) and 10 mmol sodium thiosulfate ($Na_2S_2O_3 \cdot 5H_2O$) fine powder were added. The mixture was ground for 30 min to assure a complete reaction. The reaction started readily during the mixing process, accompanied by the release of heat and evaporation of water vapor. Then, the mixture was washed with distilled water and ethanol several times to remove by-products. Finally, the product was dried at 60 °C for 2 h.

### 2.2. Characterization

The X-ray diffraction (XRD) was conducted on a MAC Science MXP18AHF X-ray diffractometer with graphite-monochromatized Cu $K_\alpha$ radiation ($\lambda = 1.54056$ Å). The product morphology was examined using transmission electron microscopy (Philips, TecnaiG220) and field emission scanning electron microscopy (JEOL, JSM-5600LV). The particle size distribution (PSD) was measured by Laser Particle Size Analyze (Malvern Zetasizer Nano S90). The BET surface area was determined by nitrogen adsorption and desorption measurements (Micromeritics ASAP 2050). The UV–vis absorption spectrum was measured on a UV–vis spectrophotometer (Hitachi U-3010). The photocatalytic experiments were conducted in an XPA-1 photochemical reactor (Xujiang Electromechanical Plant, Nanjing, China).

### 2.3. Photocatalytic test

Photocatalytic activity of the as-synthesized CdS nanoparticles was measured by the degradation of rhodamin B (RhB) under UV irridiation using a 500 W mercury lamp. Ten milligrams of photocatalysts were added to 20 mL RhB solution (Which initial concentration is 10 mg $L^{-1}$). Then the suspension was stirred for 30 min in the dark to ensure the adsorption equilibrium between the photocatalyst and the RhB. At a given illumination time, 5 mL of the suspension was collected and centrifuged to remove the photocatalyst particles, and then was analyzed by recording the UV–vis spectrum of RhB at the maximum absorption wavelength (553 nm). All the experiments were conducted at room temperature. For the sake of comparison, the photocatalytic performance of the CdS nanoparticles to methyl orange (MO) and 2, 4-Dinitrophenol were also investigated.

## 3. Results and discussion

### 3.1. Structure of CdS nanoparticles

The structure of the CdS product was evaluated by FESEM. As is shown in Fig. 1a, CdS nanoparticles were uniform. Fig. 1b is a magnified FESEM image, which reveals that the CdS product was composed of nanoparticles about 100 nm in diameter. The histogram of the particle size distribution (Fig. 1d) demonstrates that the CdS nanoparticles have relatively narrow size distribution with an average of 100 nm, which is consistent with the above FESEM analysis (Fig. 1a and b).

The crystal structure and phase of the CdS product was characterized by X-ray diffraction (XRD), as shown in Fig. 1c. The reflection peaks of the CdS product can be well indexed to the standard pattern of Hawleyite CdS (JCPDS 10-0454), confirming that pure phase of Hawleyite CdS was obtained. The broad peaks indicated the existence of small nanoparticles within the CdS product, which was in agreement with the FESEM analysis. No diffraction peaks of other impurities were detected, suggesting the CdS product with a high purity.

The nanostructure of as-synthesized CdS nanoparticles was further examined by TEM technology. Fig. 2 showed a set of TEM images for the CdS nanoparticles under different magnifications. It can be found that the CdS nanoparticles were uniform (Fig. 2a and b) with mean size of 60 nm. The magnified TEM image (Fig. 2c) also reveals that the CdS nanoparticles are loose. The inserted selected area electron diffraction (SAED) pattern in Fig. 2c further proves the polycrystalline nature of the CdS nanoparticles. Moreover, the HRTEM image (Fig. 2d) shows that the fringe spacing is 0.32 nm, corresponding well to (111) plane of CdS nanoparticles, which is in agreement with the previous results [23].

Nitrogen adsorption/desorption isotherms of the CdS nanoparticles are presented in Fig. 3. The specific surface area of the CdS nanoparticles is 78.02 $m^2/g$. According to IUPAC classification, it can be seen that, the hysteresis loop of the CdS nanoparticles is classified as type (the characteristic of mesoporous material), which were consistent with the TEM results (Fig. 2). The result proves that there are mesoporous structures existing in the CdS nanoparticles, which can provide more accessible active sites and special passages for charge transport, and then enhancing photocatalytic activity.

### 3.2. UV–vis absorption spectrum of CdS nanoparticles

The optical absorption properties of semiconductors has a much relationship with the energy band structure, which are estimated by the UV–vis absorption spectrum [24,25]. The UV–vis absorption spectrum of the CdS nanoparticles

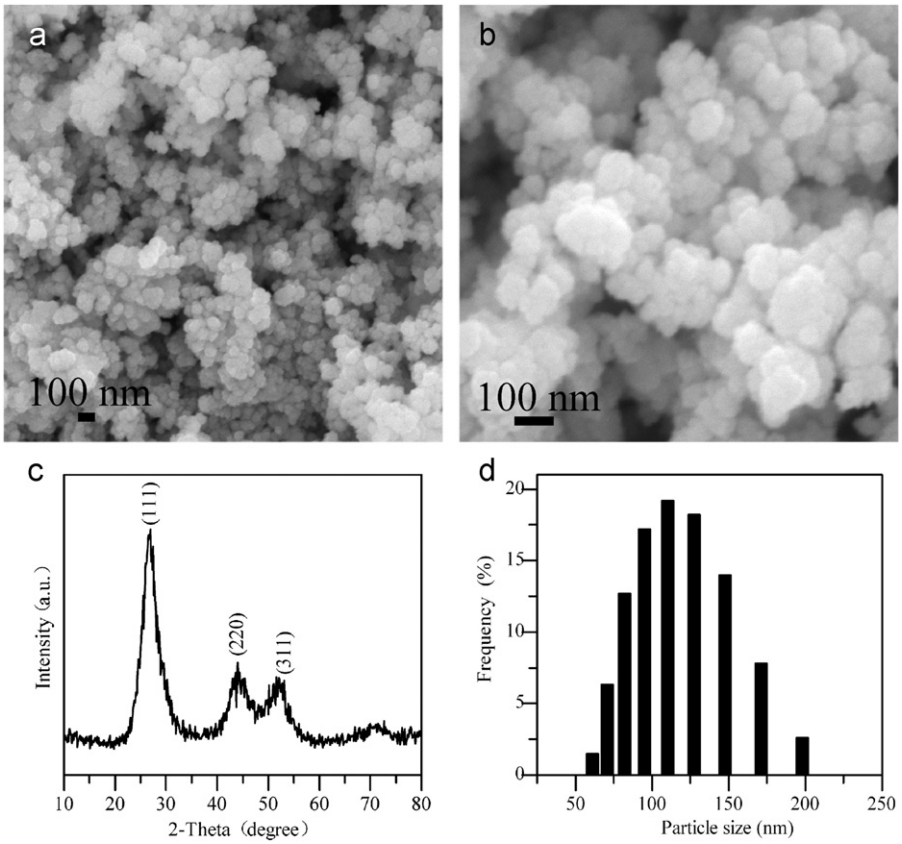


Fig. 1. FESEM images of the CdS nanoparticles (a and b), XRD pattern (c) and PSD image (d).

is shown in Fig. 4. According to the spectrum, the CdS nanoparticles present strong photoabsorption property in the UV light region, indicating promising photocatalytic activity. As for a semiconductor, the optical absorption near the band edge obeys the following equation [26]:

$$(\alpha hv)^{n/2} = A\,(hv - E_g). \quad (1)$$

where $\alpha$, $h$, $v$, $A$ and $E_g$ are the optical absorption coefficient, Plank constant, light frequency, a constant and band gap energy, respectively. Because the optical absorption coefficient ($\alpha$) is linearly proportional to the absorbance ($A$) of a sample, the intersection of the extrapolated linear portion in the plot of $(Ahv)^2$ versus the photon energy ($hv$) gives the band gap energy ($E_g$). Then the energy band gap ($E_g$) of the CdS nanoparticles was calculated to be about 2.24 eV from the onset of the absorption edge (inset of Fig. 4). It suggests that the as-synthesized CdS nanoparticles have suitable energy band gap for photocatalytic degradation of organic pollutants under UV irradiation.

### 3.3. Photocatalytic activity of CdS nanoparticles

RhB, MO and 2, 4-Dinitrophenol were selected as model organic pollutants to evaluate the photocatalytic performance of the CdS nanoparticles. Fig. 5 displayed the concentration changes of RhB, MO and 2, 4-Dinitrophenol ($C/C_0$) as a function of irridiation time. With regard to RhB, the color of the dispersion solution completely disappeared after 60 min of irradiation, and 95% of RhB was degraded. For MO, only 80% could be reached within the same period, and less than 82% of 2, 4-Dinitrophenol was degraded during this interval. The above results can be attributed to that different dye molecules have different adsorption characteristics on CdS nanoparticles [27]. Hence, the CdS nanoparticles exhibit higher photocatalytic activity on RhB than that of MO and 2, 4-Dinitrophenol. The RhB was chosen for a detailed study of the photocatalytic activity over CdS nanoparticles.

In order to investigate the photocatalytic activity of the CdS nanoparticles, a series of photocatalytic experiments were performed. Fig. 6a shows the temporal evolution of RhB absorbance spectra on the CdS nanoparticles at different irradiation intervals. It can be noted that, the intensity of absorption peak at 553 nm decreased rapidly when prolonging the irradiation time. The absorption peak completely disappearred after irradiating for 60 min, indicating the complete degradation of RhB. The result shows that the CdS nanoparticles have excellent photocatalytic performance. No new absorption peaks appears in the spectrum, suggesting that the photocatalytic degradation of RhB has occurred.

In order to thoroughly measure the photocatalytic activity of the CdS nanoparticles, the concentration changes of RhB

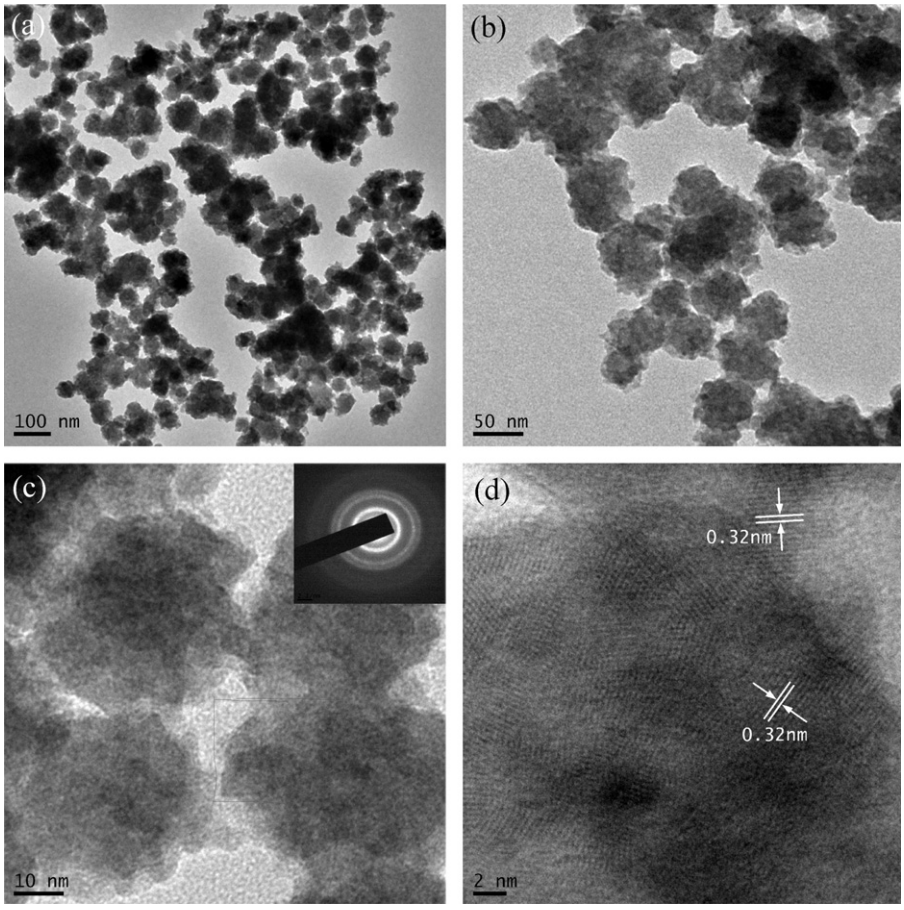


Fig. 2. TEM images of the CdS nanoparticles (a–c), SAED pattern (inset of c) and HRTEM image (d).

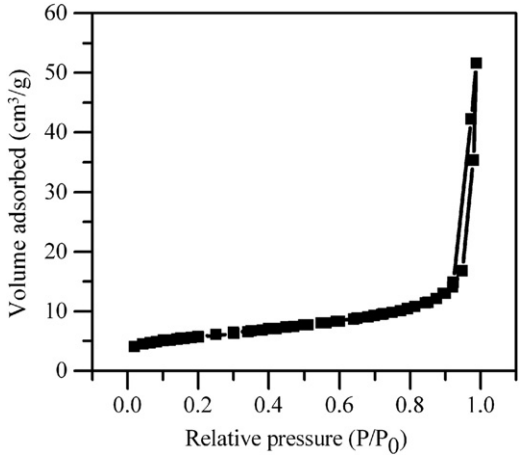


Fig. 3. The nitrogen adsorption–desorption isotherms of the CdS nanoparticles.

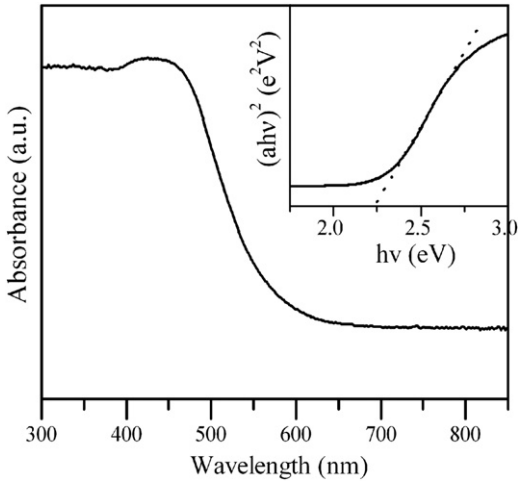


Fig. 4. The UV–vis absorption spectrum of the CdS nanoparticles.

($C/C_0$) at 553 nm as a function of irridiation time are shown in Fig. 6b. Here, $C_0$ and $C$ are the dye concentration before and after irridiation, respectively. Without photocatalyst, no obvious degradation of RhB was observed as the time prolonged. It proved that the pure photolysis of RhB can be neglected, which is very important in view of the practical application. As a comparison, P25 (which had been regarded as a wide and efficient photocatalyst under UV irridiation [28]) was also used to evaluate the photocatalytic performance of the CdS nanoparticles. While, it is noting that 95% of RhB was degraded within 60 min of irradiation by the CdS nanoparticles, whereas that of P25 was 90%. Hence, the photocatalytic activity of the CdS nanoparticles was slightly higher than that of P25, which is in consistent with the

reported literature [29]. Comparing with the previously reported degradation of the same dye (RhB) in the presence of CdS, For example, Guo et.al obtained CdS quantum dots by reflux routine, and 15% of RhB was degraded within 60 min of irradiation by the CdS quantum dots [30], which was much lower than that of the as-synthesized CdS nanoparticles. Therefore, the as-synthesized CdS nanoparticles can act as an efficient photocatalyst.

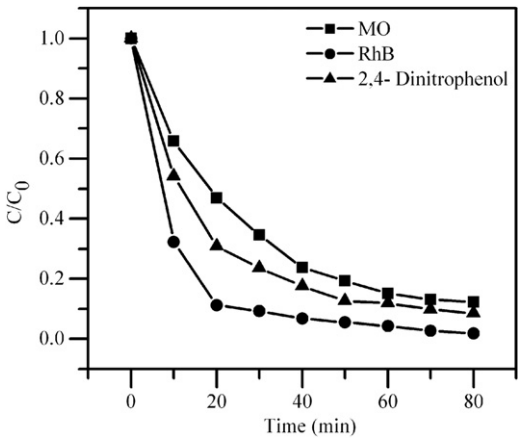


Fig. 5. The concentration changes of RhB, MO and 2, 4-Dinitrophenol ($C/C_0$) as a function of irridiation time.

The photocatalytic activity was affected by many factors, such as specific surface area and microstructure. As shown in Fig. 3, the specific surface area of the CdS nanoparticles (78.02 $m^2/g$) is bigger than that of the P25 (45.01 $m^2/g$). Hence, the CdS nanoparticles could exhibit an enhanced photocatalytic activity. On the other hand, the excellent photocatalytic activity is in close relation with the microstructure of the as-synthesized CdS nanoparticles. Comparing with P25, the better photocatalytic ability of the CdS nanoparticles is possibly arising from its nanostructure. It is observed (Fig. S1 in the Supporting Information) that P25 was composed of nanoparticles about 80 nm in diameter, and had a serious aggregation. While, the CdS nanoparticles were uniform (Figs. 1 and 2) with mean size of 60 nm, and have relatively narrow size distribution. Hence, the uniform CdS nanostructures can provide a facile path for efficient transport of electrons. As a result, the photogenerated electron–hole pairs could move effectively to the surface and then degrade RhB molecules, enhancing the photocatalytic efficiency [31].

In order to quantitatively understand the reaction kinetics of RhB degradation, we apply the pseudo-first-order model [32] expressed as follows, $\ln(C_0/C)=kt$, where, $C_0$ and $C$ are the dye concentration before and after irradiation, respectively, $k$ is the pseudo-first order reaction rate constant. Fig. 6c depicts the photocatalytic

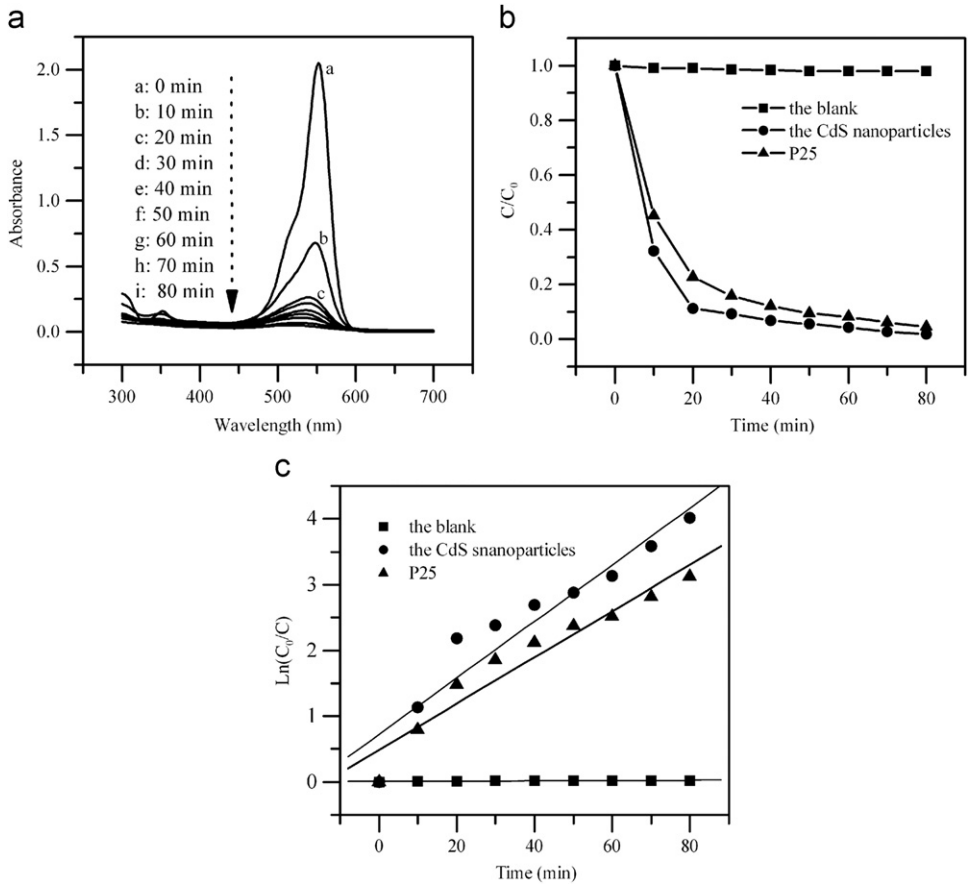


Fig. 6. (a) The temporal evolution of RhB absorbance spectra in the presence of the CdS nanoparticles under UV irridiation at different intervals. (b) Concentration changes of RhB ($C/C_0$) at 553 nm as a function of irridiation time. (c) In $C_0/C$ versus irridiation time in RhB solution.

Table 1
Kinetic constants, regression coefficients and the kinetics equations for the degradation of RhB over the samples under UV irridiation.

| Samples | $k$ ($min^{-1}$) | $R^2$ | Kinetics equation |
|---|---|---|---|
| CdS nanoparticles | 0.04299 | 0.95164 | $Y=0.7231+0.04299X$ |
| P25 | 0.03517 | 0.96541 | $Y=0.4875+0.03517X$ |
| Blank | 0.00574 | 0.89226 | $Y=2.26194E\text{-}4+0.00574X$ |

degradation kinetics of RhB based on the data plotted in Fig. 6b. As is shown in Fig. 6c, $k$ values for the CdS nanoparticles, P25 and the blank are 0.04299 $min^{-1}$, 0.03517 $min^{-1}$ and 0.00574 $min^{-1}$, respectively. The above results reveal that the $k$ value for the CdS nanoparticles is higher than that of P25, indicating that the CdS nanoparticles holds higher photocatalytic activity than that of P25. Their linearly dependent coefficients ($R$) and the kinetics equations were presented in Table 1, suggesting a rather good correlation to the pseudo-first-order reaction kinetic.

## 4. Conclusions

In summary, CdS nanoparticles (about 60 nm in diameter and the specific surface area is 78.02 $m^2/g$) have been successfully obtained by a simple one-step solid-state reaction. The as-synthesized CdS nanoparticles possessed excellent photocatalytic activity, which has higher photocatalytic efficiency than that of P25 and reported CdS. This study not only provided a low-cost, simple approach for a large-scale production of CdS in industry, but also demonstrated that the CdS nanoparticles prepared by this routine exhibit excellent photocatalytic activity.

## Acknowledgments

This work was financially supported by the Natural Science Foundation of Xinjiang University (No. BS100129), the Excellent Doctor Innovation Program of Xinjiang University (No. XJUBSCX-2011004), the National Natural Science Foundation of China (Nos. 21101132 and 21061013), the Xinjiang Autonomous Region with Science and Technology Project Plan (No. 200991101), the Autonomous Regions High Technology Research and Development Program (No. 201016118) and the Program for Changjiang Scholars and Innovative Research Team in University of Ministry of Education of China (IRT1081).

## Appendix A. Supporting information

Supplementary data associated with this article can be found in the online version at http://dx.doi.org/10.1016/j.ceramint.2012.07.098.

## References

[1] M. Ahmad, Y. Shi, A. Nisar, H. Sun, W. Shen, M. Wei, J. Zhu, Synthesis of hierarchical flower-like ZnO nanostructures and their functionalization by Au nanoparticles for improved photocatalytic and high performance Li-ion battery anodes, Journal of Materials Chemistry 21 (2011) 7723–7729.
[2] C. Suwanchawalit, S. Wongnawa, P. Sriprang, P. Meanha, Enhancement of the photocatalytic performance of Ag-modified $TiO_2$ photocatalyst under visible light, Ceramics International 38 (2012) 5201–5207.
[3] M.H. El-Naas, S.A. Al-Muhtaseb, S. Makhlouf, Biodegradation of phenol by *Pseudomonas putida* immobilized in polyvinyl alcohol (PVA) gel, Journal of Hazardous Materials 164 (2009) 720–725.
[4] J.C. Hu, Z. Song, L.F. Chen, H.J. Yang, J.L. Li, R. Richards, Adsorption properties of MgO (111) nanoplates for the dye pollutants from wastewater, Journal of Chemical and Engineering Data 55 (2010) 3742–3748.
[5] S. Cho, J.W. Jang, J. Kim, J.S. Lee, W. Choi, K.H. Lee, Three-dimensional Type II ZnO/ZnSe heterostructures and their visible light photocatalytic activities, Langmuir 27 (2011) 10243–10250.
[6] Q. Xiang, G.F. Meng, H.B. Zhao, Y. Zhang, H. Li, W.J. Ma, J.Q. Xu, Au nanoparticle modified $WO_3$ nanorods with their enhanced properties for photocatalysis and gas sensing, Journal of Physical Chemistry C 114 (2010) 2049–2055.
[7] J. Zhang, S.W. Liu, J.G. Yu, M. Jaroniec, A simple cation exchange approach to Bi-doped ZnS hollow spheres with enhanced UV and visible-light photocatalytic $H_2$-production activity, Journal of Materials Chemistry 21 (2011) 14655–14662.
[8] J.B. Joo, Q. Zhang, I. Lee, M. Dahl, F. Zaera, Y.D. Yin, Mesoporous anatase titania hollow nanostructures though silica-protected calcination, Advanced Functional Materials 22 (2012) 166–174.
[9] X.J. Liu, L.K. Pan, T. Lv, G. Zhu, Z. Sun, C.Q. Sun, Microwave-assisted synthesis of CdS-reduced graphene oxide composites for photocatalytic reduction of Cr(vi), Chemical Communications 47 (2011) 11984–11986.
[10] B.T. Raut, M.A. Chougule, S.R. Nalage, D.S. Dalavi, S. Mali, P.S. Patil, V.B. Patil, CSA doped polyaniline/CdS organic–inorganic nanohybrid: physical and gas sensing properties, Ceramics International 38 (2012) 5501–5506.
[11] P.G. Chavan, S.S. Badadhe, I.S. Mulla, M.A. More, D.S. Joag, Synthesis of single crystalline CdS nanocombs and their application in photo-sensitive field emission switches, Nanoscale 3 (2011) 1078–1083.
[12] Z. Khan, M. Khannam, N. Vinothkumar, M. De, M. Qureshi, Hierarchical 3D NiO–CdS heteroarchitecture for efficient visible light photocatalytic hydrogen generation, Journal of Materials Chemistry 22 (2012) 12090–12095.
[13] Q. Li, B.D. Guo, J.G. Yu, J.R. Ran, B.H. Zhang, H.J. Yan, J.R. Gong, Highly efficient visible-light-driven photocatalytic hydrogen production of CdS-cluster-decorated graphene nanosheets, Journal of the American Chemical Society 133 (2011) 10878–10884.
[14] J. Cai, J. Jie, P. Jiang, D. Wu, C. Xie, C. Wu, Z. Wang, Y. Yu, L. Wang, X. Zhang, Q. Peng, Y. Jiang, Tuning the electrical transport properties of n-type CdS nanowires via Ga doping and their nano-optoelectronic applications, Physical Chemistry Chemical Physics 13 (2011) 14663–14667.
[15] W.M. Wu, G.D. Liu, Q.H. Xie, S.J. Liang, H.R. Zheng, R.S. Yuan, W.Y. Su, L. Wu, A simple and highly efficient route for the preparation of p-phenylenediamine by reducing 4-nitroaniline over commercial CdS visible light-driven photocatalyst in water, Green Chemistry 14 (2012) 1705–1709.
[16] M. Luo, Y. Liu, J.C. Hu, H. Liu, J.L. Li, One-pot synthesis of CdS and Ni-Doped CdS hollow spheres with enhanced photocatalytic activity and durability, ACS Applied Materials and Interfaces 4 (2012) 1813–1821.
[17] J. Zhang, Y.H. Wang, Z. Lin, F. Huang, Formation and self-assembly of cadmium hydroxide nanoplates in molten composite-hydroxide solution, Crystal Growth and Design 10 (2010) 4285–4291.
[18] Z.G. Li, J.H. Sui, X.L. Li, W. Cai, Oriented attachment growth of quantum-sized CdS nanorods by direct thermolysis of single-source precursor, Langmuir 27 (2011) 2258–2264.

[19] H. Qi, J.F. Huang, L.Y. Cao, J.P. Wu, D.Q. Wang, One-dimensional CuS microstructures prepared by a PVP-assisted microwave hydrothermal method, Ceramics International 38 (2012) 2195–2200.
[20] Y. Cao, D. Jia, J. Zhou, Y. Sun, Simple solid-state chemical synthesis of $ZnSnO_3$ nanocubes and their application as gas sensors, European Journal of Inorganic Chemistry 2009 (2009) 4105–4109.
[21] Z.P. Sun, L. Liu, L. Zhang, D.Z. Jia, Rapid synthesis of ZnO nanorods by one-step, room-temperature, solid-state reaction and their gas-sensing properties, Nanotechnology 17 (2006) 2266–2270.
[22] Y. Zong, Y.L. Cao, D.Z. Jia, P.F. Hu, The enhanced gas sensing behavior of porous nanocrystalline $SnO_2$ prepared by solid-state chemical reaction, Sensors and Actuators B 145 (2010) 84–88.
[23] Y. Guo, H. Zhang, Y. Wang, Z.L. Liao, G.D. Li, J.S. Chen, Controlled growth and photocatalytic properties of CdS nanocrystals implanted in layered metal hydroxide matrixes, Journal of Physical Chemistry B 109 (2005) 21602–21607.
[24] M. Shang, W.Z. Wang, J. Ren, S.M. Sun, L. Zhang, A novel $BiVO_4$ hierarchical nanostructure: controllable synthesis, growth mechanism, and application in photocatalysis, CrystEngComm 12 (2010) 1754–1758.
[25] R. Hao, X. Xiao, X.X. Zuo, J.M. Nan, W.D. Zhang, Efficient adsorption and visible-light photocatalytic degradation of tetracycline hydrochloride using mesoporous BiOI microspheres, Journal of Hazardous Materials 209 (2012) 137–145.
[26] F. Duan, Y. Zheng, M. Chen, Flowerlike $PtCl_4/Bi_2WO_6$ composite photocatalyst with enhanced visible-light-induced photocatalytic activity, Applied Surface Science 257 (2011) 1972–1978.
[27] S.B. Khan, M. Faisal, M.M. Rahman, A. Jamal, Exploration of $CeO_2$ nanoparticles as a chemi-sensor and photo-catalyst for environmental applications, Science of the Total Environment 409 (2011) 2987–2992.
[28] N. Yao, C.C. Wu, L.C. Jia, S. Han, B. Chi, J. Pu, L. Jian, Simple synthesis and characterization of mesoporous (N, S)-codoped $TiO_2$ with enhanced visible-light photocatalytic activity, Ceramics International 38 (2012) 1671–1675.
[29] T.T. Yang, W.T. Chen, Y.J. Hsu, K.H. Wei, T.Y. Lin, T.W. Lin, Interfacial charge carrier dynamics in core–shell Au–CdS nanocrystals, Journal of Physical Chemistry C 114 (2010) 11414–11420.
[30] Y.M. Guo, L.L. Wang, L. Yang, J. Zhang, L. Jiang, X.M. Ma, Optical and photocatalytic properties of arginine-stabilized cadmium sulfide quantum dots, Materials Letters 65 (2011) 486–489.
[31] G.H. Tian, Y.J. Chen, W. Zhou, K. Pan, Y.Z. Dong, C.G. Tian, H.G. Fu, Facile solvothermal synthesis of hierarchical flower-like $Bi_2MoO_6$ hollow spheres as high performance visible-light driven photocatalysts, Journal of Materials Chemistry 21 (2011) 887–892.
[32] J.Z. Yang, J.W. Yu, J. Fan, D.P. Sun, W.H. Tang, X.J. Yang, Biotemplated preparation of CdS nanoparticles/bacterial cellulose hybrid nanofibers for photocatalysis application, Journal of Hazardous Materials 189 (2011) 377–383.